Guiding safe and sustainable technological innovation under uncertainty: a case study of III-V/silicon photovoltaics

Blanco Rocha, C.F.

Chapter 5

Probabilistic and prospective ecological risk assessment of III-V/silicon tandem photovoltaics

III-V/silicon tandem solar cells offer one of the most promising avenues for high-efficiency, high-stability photovoltaics. However, a key concern is the potential environmental release of group III-V elements, especially arsenic. To inform long-term policies on the energy transition and energy security, we develop and implement a framework that fully integrates future PV demand scenarios with dynamic stock, emission and fate models in a probabilistic ecological risk assessment. We examine three geographical scales: local (including a floating utility-scale PV and waste treatment); regional (city-wide) and continental (Europe). Our probabilistic assessment considers a wide range of variations for over one hundred uncertain technical, environmental and regulatory parameters. We find that significant III-V/silicon PV penetration in energy grids at all scales presents low-to-negligible risks to soil and freshwater organisms. Risks are further abated if recycling is considered at the panels' end-of-life.

Keywords: III-V/silicon cells; risk assessment; toxicity; photovoltaics; safe-by-design; sustainable innovation

This chapter is based on the manuscript *High-efficiency III-V/Si tandem solar cells pose low toxicity risks to soil and freshwater ecosystems* (Blanco, C.F., Quik, J.T.K., Hof, M., Behrens, P., Cucurachi, S., Peijnenburg, W.J.G.M., Dimroth, F., Vijver, M.G.). In preparation for submission to *Energy Environ. Sci.*

5.1. Introduction

Recent decades have seen a dramatic increase in photovoltaic electricity (PV) in energy markets worldwide.[1] Next to lower manufacturing costs, a key driver for increased PV adoption has been the environmental benefits when compared to fossil and nuclear-based electricity generation.[2,3] An important factor for the success of the currently dominating crystalline silicon (c-Si) PV technologies is that silicon has low toxicity[4]. This has set a benchmark against which emerging PV technologies such as III-V/silicon tandem cells (III-V/Si) would be judged. III-V/Si tandem cells stack thin light-absorbing layers of Group III and V elements (gallium, indium, arsenide, phosphide) on top of a c-Si wafer to achieve record-breaking conversion efficiencies for non-concentrating systems that can exceed 35%.[5] Manufacturing III-V/Si with current technology is very expensive and important research efforts are underway to make them more economically attractive.[6–9] However, concerns regarding potentially toxic releases of III-V metals and metalloids to the environment could hinder investment and stall further development and deployment of the technology. As a result, III-V/Si may miss out on important cost-reductions that could be achieved via technological breakthroughs and/or learning by doing.

Investigating the potential environmental impacts and risks of innovative PV designs such as III-V/Si during early research and development stages can assist in making designs more competitive from an environmental perspective.[10–12] The environmental impacts of emerging PV technologies have often been assessed in a prospective way using life cycle assessment (LCA) with future projections.[13] Blanco et al.[14] recently investigated the LCA impacts of commercially viable III-V/Si cell concepts and concluded that they could perform similar or better than silicon PV across most environmental impact categories, including climate change, fresh water ecotoxicity, eutrophication, and others. The LCA approach, however, only allows a comparison of impact indicators in a relative sense, where environmental emissions are aggregated across space and time.[15] To determine whether the emissions pose actual risks, they must be evaluated in a specified temporal and spatial context. Such an evaluation can be performed by means of ecological risk assessment.[16] However ecological risk assessments for emerging technologies are challenging from a modelling and data availability perspective and have not been conducted so far for III-V/Si PV systems. In this study we address this important knowledge gap by assessing the ecological risks of metal and metalloid releases that may take place during the life cycle of III-V/Si PV systems.

Recent studies of toxicity of emerging PV technologies have a large degree of heterogeneity and focus selectively on single or small subsets of PV system components, life-cycle stages, release mechanisms and/or toxicity endpoints.[17–20] To avoid these shortcomings, we adopt a comprehensive approach by screening for relevant emissions in all life-cycle stages of III-V/Si panels and estimating the risks posed by these emissions in plausible and well-defined PV demand scenarios at three geographical scales: local, regional and continental. Furthermore, we recognize that a holistic and forward-looking assessment such as this introduces numerous and large uncertainties and variabilities.[21]

We therefore use a probabilistic risk assessment approach to explicitly consider these in an integrated PV demand-emission-fate model and quantify uncertainty in the outcomes of the assessment, i.e., risk indicators.[22] We then use global sensitivity analysis to reveal which factors contribute most to this uncertainty. While the III-V/Si technology is still in development, this information is equally or more important than the magnitude of the risk indicators, as it can help prioritize further research and development of the technology as well as simplify the assessment by disregarding trivial uncertainties and variabilities.

5.2. Methods

5.2.1. Overview of modelling framework

To assess the ecological risks from III-V/Si panels in future PV demand scenarios we developed an integrated model that consists of five steps. First, demand for installed PV capacity (in MW or GW) over a one-hundred-year modelling period (2031-2130) is determined for each geographical scale (continental, regional, local) based on relevant PV demand scenarios and stated policies (section 5.2.2). Second, a dynamic stock model is used to determine the amount of PV panels that would be manufactured, installed, operated, recycled and discarded each year in order to satisfy the demand required in the previous steps, while accounting for accidental panel breakage and panels reaching the end of their useful life (section 5.2.3). Third, potential releases of arsenic, gallium and indium (direct emissions) from PV panels to the environment at each life-cycle stage are calculated with a specific emission model developed for each release mechanism (section 5.2.4). Fourth, the environmental distribution and fate of the emitted masses across different environmental compartments (soil, freshwater, air) in each year is determined using a dynamic fate model. Predicted environmental concentrations (PEC) in each compartment are then calculated from the resulting mass in each compartment and the compartment's volume (section. 5.2.5). Finally, a risk quotient (RQ) is calculated as the ratio of PEC to the predicted no-effect concentration (PNEC) that has been reported in literature for each compartment (section 5.2.6).

All components of the model allow for the consideration of probability distributions for input parameters. The model's input parameter descriptions and the corresponding distributions used in this case study are reported in Appendix Table A.4-1. Further details on calculations and assumptions for each step are also documented in Appendix Section A.4. The model was built on the statistical software *R* supported by macro-enabled Microsoft Excel spreadsheets. The annotated *R* scripts and Excel spreadsheets are available for download in https://github.com/jormercury/solar-simplebox.

5.2.2. Demand projections

In the first step we determined the quantity of installed III-V/Si panels required to meet PV electricity demand scenarios for three geographical scales:

- *SKY_EUR,* a continental scale where we based future PV demand on the Shell Sky Scenario[23] for Europe, which is the most ambitious with regards to electrification and future participation of PV from the Shell family of scenarios. We combined the Sky projections for total PV demand with the IEA's "High GaAs" scenario, in which III-V cells comprise 5% of the distributed and 15% of the utility-scale PV demand.[24]
- *RES_AMS,* a regional scale representing the city of Amsterdam and based on the municipality's stated ambitions in their Regional Energy Strategy (RES v1.0)[25]. Here we also applied III-V/Si market shares from the IEA "High GaAs" scenario.
- *UTI_LOC*, a local scale reflecting a utility PV plant consisting of 50 MW of floating III-V/Si panels installed on a lake area of 0.9 km^2 in addition to 50,000 distributed panels (14 MW) installed on rooftops in the surrounding area and draining towards the lake. End-of-life (EOL) PV treatment is also assumed to take place within this area. As such the local scale is meant to represent an unlikely worst-case scenario for the local water compartment.*

The growth in installed PV capacity over the period 2031-2130 in both the SKY_EUR and the RES_AMS scenarios were modelled using logistic-growth curves. In SKY_EUR, we assumed an initial capacity addition of 100 MW_p and stabilizing at 430 GW_p. We took an annual growth rate of 14.1% from the 75th percentile of 1100 different PV deployment scenarios in Europe that were reviewed and harmonized by Jaxa-Rozen et. al.[26] In the RES_AMS scenario we assumed an initial capacity addition of 0.1 MW_p in the year 2031 and stabilizing at 110 MW_p following a higher growth rate of 20%. For the UTI_LOC scenario the amounts of PV panels installed were kept constant throughout the modelling period, with replacement of broken panels and those that reach their EOL.

With an expected 28% panel conversion efficiency, III-V/Si panels will have a rating of 280 W_p per m^2 of panel. Thus, every 1 MW_p of planned installed capacity would require a PV installation with an effective area of 3,571 m^2.

5.2.3. Dynamic stock flows

Yearly stock flows of III-V/Si panels (quantified as m^2 of PV panel) were calculated using a dynamic stock model[27–29] for a one-hundred year modelling period. In the stock model, additional panels are manufactured each year to meet the increasing demand, to replace broken panels, and to replace panels that reached the end of their useful life (due to long-term degradation). In lieu of specific panel lifetime data, we assumed a normal distribution for III-V/Si panel lifetime of each yearly cohort centred at 30 years and with a standard deviation of 5. Accidental panel breakage rates of 0.06-0.12%/year were taken based on panel crack statistics reported by the International Energy Agency.[30]

* In their Regional Energy Strategy, the Amsterdam municipality has marked floating PV as a last resort, only to take place if the regional and national goals cannot be satisfied with installation on rooftops and other public infrastructure.

5.2.4. Emissions of III-V metals and metalloids

Based on III-V/Si cell design specifications proposed by a European project[31], each m^2 of panel would contain 8.81 g of arsenic (As), 15.06 g of gallium (Ga) and 0.1 g of indium (In).[31] The As, Ga and In content in each panel is subject to environmental release depending on the specific conditions and dissolution processes that can take place during manufacturing, operation (use phase), end-of-life (EOL) phase (Figure 5-1).

Manufacturing. III-V substances enter the supply chain of III-V/Si cells in the metalorganic vapour phase epitaxy process (MOVPE) which is used to grow the absorber III-V layers on top of the silicon wafer. These substances are supplied from hydride gases and metalorganic precursors (arsine, trimethylgallium and trimethylindium). The fraction not deposited on the solar cells is distributed in two waste streams: a gas stream that is captured by a scrubber, and a solid stream composed of materials that deposit on the different elements of the reactor and on filters which are cleaned periodically. In the scrubber, a dry zeolite/copper-based granulate adsorbs the toxic substances.

The current best practice in the industry is to reintroduce the used scrubber granulate into the smelting process for copper, in which case the III-V content is captured as an acceptable impurity in the metal. It is likely that the valuable metals (indium, gallium) will be eventually separated and recovered. For arsenic there is no economic case at present, however there is technical feasibility for arsenic recovery from the used adsorbent granulates. Such recoveries may become economically viable when the arsenic content in waste is sufficient (e.g., ~100 ton/year)[†]. Recovery may also be driven by resource scarcity of critical materials like indium and gallium.[32] Recovery processes will have an associated efficiency, typically between 95-99%, and the remaining fraction (rejects) would be disposed in an underground hazardous waste storage facility.

The solid waste stream from MOVPE that deposits in the reactor is periodically removed as a standard cleaning procedure. This waste is also discarded in an underground hazardous waste storage facility. These types of facilities in Europe are typically installed on sealed and carefully monitored abandoned mine shafts, where potential migration of contaminants is deemed implausible.

Use phase (operation). Two processes were modelled to estimate potential releases during operation: dissolution at the cracked surface of III-V materials directly exposed to rain, and transport of III-V materials on non-exposed parts that get dissolved by water ingress and are transported to the crack where it is then released. We modelled the former process following the method proposed by Celik et al.[33], which is based on an application of the Noyes-Whitney equation[34]. The latter process was modelled using equations 5-1 and 5-2, where $trans_{crack}$ is the transport of dissolved metal to the crack (g/s), J_{crack} is the flux of dissolved metal to the crack (g/m^2/s), D is the diffusion coefficient of metal (m^2/s), C_s is the saturated mass concentration of metal in water in g/m^3, C_b is the concentration of

[†] Personal communication from UMICORE.

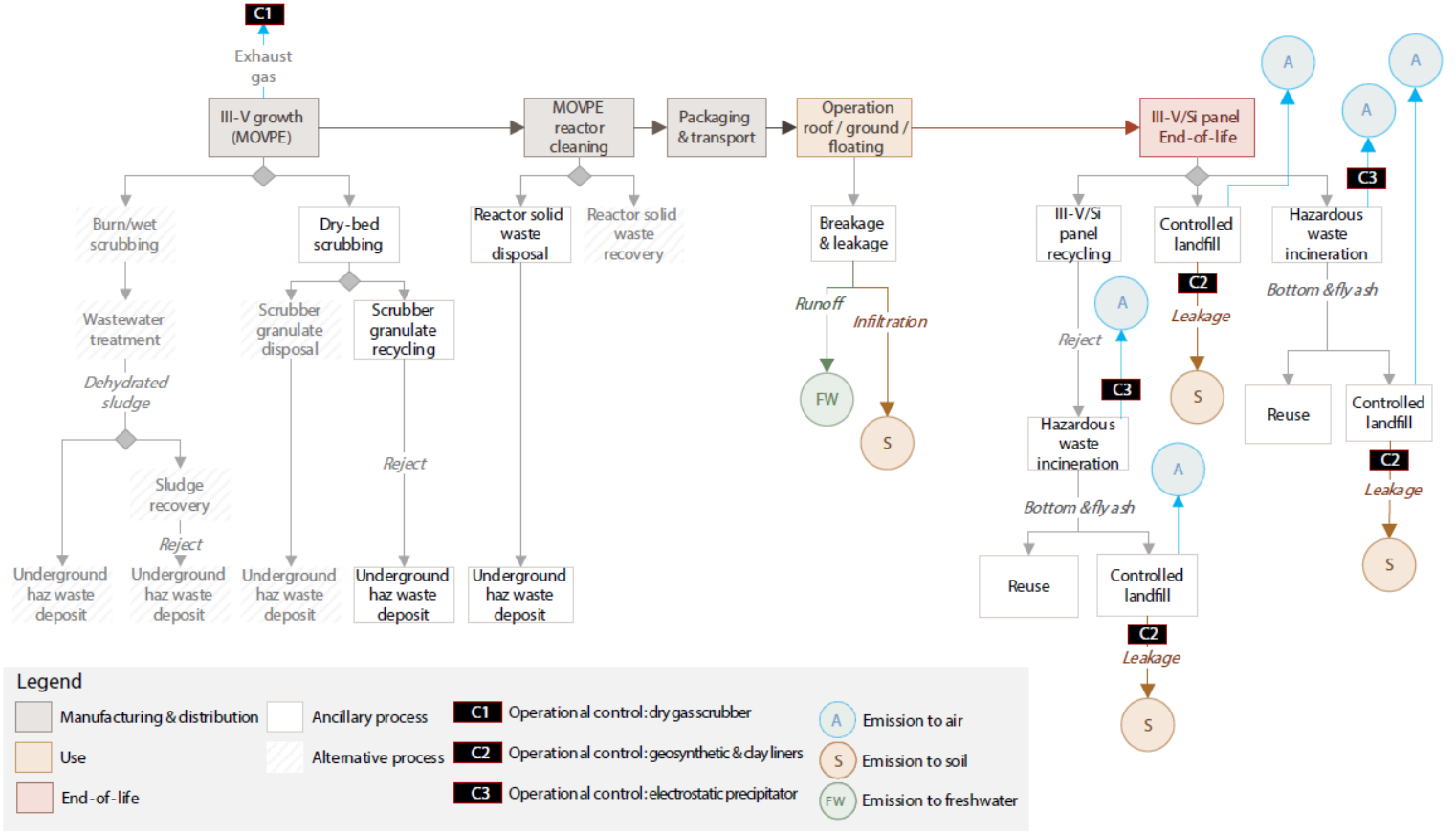

Figure 5-1 Identification of potential sources of III-V emissions in the life cycle of III-V/Si PV panels

metal in bulk solvent (rainwater) in g/m^3, and $distance_{cr}$ is the average travel distance of the metal from any point in the panel to the crack (m), calculated using the method of Mathai et al.[35] Cracked panels were assumed to leach for one year after which they would be replaced.

$$trans_{crack} = J_{crack} \cdot A_{cr\_side} \quad \text{(Eq. 5-1)}$$

$$J_{crack} = D \cdot \frac{Cs - Cb}{distance_{cr}} \quad \text{(Eq. 5-2)}$$

End-of-life phase: Recycling. The European Waste Management Directive for electronic products -including photovoltaic panels- requires that 85% is collected for treatment and preparation for reuse/recycling.[36] It is likely, however, that the panels are disassembled to recover the easily recyclable materials such as aluminium and glass.[‡] We modelled two scenarios for each scale: with and without recovery of III-V materials. In former case we assumed recovery efficiencies for these processes based on existing patents and published recycling methods for similar technologies[37–39].

End-of-life phase: Incineration. In incineration facilities, it has been found that 20-80% of arsenic in waste may remain in the bottom ash while the rest is volatized.[40] The volatized fraction is directed to emission control mechanisms at the stack such as electrostatic precipitators (ESP) with removal efficiencies that typically range between 99.5-99.9%.[41] Arsenic that is not vaporised in the incinerated panels is emitted to air and the remaining fraction is collected as secondary waste with bottom ash, fly ash and filters. Gallium and indium do not form volatile organic compounds, so we assumed 100% remains in the bottom ash. In Europe, secondary waste from incineration facilities is typically either sent to a controlled landfill or reused in construction material.[42]

End-of-life phase: landfill. Two main processes drive emissions from landfilled PV waste: leaching from the waste to the leachate within the landfill, and leakage of the leachate from the landfill to the surrounding soil. The former will be largely regulated by a waste/leachate partitioning coefficient (k_W) which can be determined empirically from leaching tests or field measurements. Leaching and subsequent leakage from the landfill will also be largely regulated by the effective infiltration (I), the amount of rainfall that infiltrates and passes through the landfill's containment structures such as clay or geosynthetic liners. We use a simplified version of EPA's Composite Model for Leachate Migration with Transformation Products (EPACMTP)[43], where the mass balance for a landfill cell is given by equations 5-3 and 5-4.

$$A_W \cdot D_{LF} \cdot \rho_W \cdot \frac{dC_w}{dt} = A_W \cdot I \cdot C_L(t) \quad \text{(Eq. 5-3)}$$

$$C_L(t) = K_W \cdot C_W(t) \quad \text{(Eq. 5-4)}$$

When modelling emissions we took a conservative approach and assumed that all III-V elements in the PV cells are fully soluble. This is a common starting point for metals risk

[‡] Ibid.

assessment within the EU.[44] Another important consideration is that, once released, metals and metalloids can exist in different forms like organic complexes with dissolved organic matter, inorganic complexes with dissolved anions, or free hydrated metal ions. This applies especially to arsenic, which can exist in four oxidation states with different toxicities: –3, 0, +3, and +5. In this study, we assume that arsenic dissolves entirely to its most toxic form (*arsenite*, +3). Indium and gallium may also exist in different oxidation states, but once released to the environment tend to revert to their +3 oxidation state.[45]

5.2.5. Predicted environmental concentrations

We then modelled the distribution of the emitted III-V substances in the environment using SimpleBox v4, a widely used tool for fate modelling developed by the Netherlands Institute of Public Health and the Environment (RIVM).[46] For the SKY_EUR continental scale we used the landscape settings for the European continent that were established for the European Union System for the Evaluation of Substances (EUSES).[47] In the SimpleBox model, the continental scale contained the regional AMS_RES scale embedded, which in turn contained the embedded local UTI_LOC scale (SimpleBox calculates exchanges between embedded scales). To model the regional AMS_RES and UTI_LOC landscape we derived surface water and soil coverage data from GIS data made available by the Amsterdam municipality[48], and weather data provided by the Royal Netherlands Meteorological Institute (KNMI)[49].

To conduct dynamic PEC calculations we coupled a probabilistic implementation of the SimpleBox model using the @Risk add-in (Palisade, v8.1.0) with the deSolve[72] package in R. SimpleBox is based on the original implementation as described in Schoorl et al.[46,50] with the addition of a local scale with an air, soil, water and sediment compartment based on van de Meent et al.[51] In this implementation, the model matrix of all rate constants is read from the SimpleBox Excel spreadsheets and combined with the annual III-V emissions (calculated in section 5.2.4), using the event function in deSolve.

5.2.6. Predicted no-effect concentrations and risk quotients

We took the PNEC values recommended by the European Chemicals Agency (ECHA) in the registration dossiers for each substance.[52–54] Depending on each case, these were derived by ECHA from EC10 or EC50 (concentration at which 10% or 50% of the target organism presents the observed effect), LC50 (lethal concentration for 50% of the observed organisms) and LOEC (lowest observed effect concentration) values reported in literature. An assessment factor is applied to account for uncertainty in extrapolation from lab to field results, or for the limited availability of datapoints.[55]

Arsenic. The PNEC value recommended by ECHA for freshwater organisms is 5.6 μg/L, after application of an assessment factor of 3. For soil, the recommended PNEC is 2.9 mg/kg soil (dry weight) after an assessment factor of 2 has been applied.

Gallium. One NOEC for freshwater organisms was reported in the ECHA database of 10,300 μg/L.[52] Following ECHA guidelines[55], an assessment factor of 100 should be

applied for a single NOEC value, resulting in a PNEC of 103 µg/L. There was only one datum for soil organisms reported in literature, an EC50 of 0.271 g/kg soil (dw) for rice plants in acidic soil (no effects were observed in neutral soils).[56] Applying an assessment factor of 100 gives a PNEC of 2.7E-3 g/kg soil (dw). For soil, ECHA recommends using the Equilibrium Partitioning Method as an alternative calculation method when only one datum is available and choosing the lowest PNEC obtained from both methods. The Equilibrium Partitioning Method uses the PNEC in water to estimate PNEC in soil according to Equation 5-5:

$$PNEC_{soil} = \frac{K_{sw}}{\rho_{soil}} \cdot PNEC_{water} \cdot 1000 \qquad \text{(Eq. 5-5)}$$

In Equation 5-5, K_{sw} is the soil water partition coefficient for gallium and ρ_{soil} is the density of soil phase, 2500 kg/m^3. This would result in a PNEC of 4E-2 g/kg soil (dw). We therefore take the lower PNEC of 2.7E-3 g/kg soil (dw).

Indium. The toxicity data for indium (In3+) were taken from the ECHA database, which recommends a PNEC of 40.6 µg/L after applying an assessment factor of 3. For terrestrial organisms, the recommended value is 7.3E-3 g/kg soil (dw), after applying an assessment factor of 10.[53].

RQs for each compartment were calculated as the PEC/PNEC ratio, where RQ values approaching or exceeding 1 indicate a potential situation of concern.

5.2.7. Uncertainty and sensitivity analysis

We used the Monte Carlo uncertainty propagation method[57] to determine uncertainty in the PECs and RQs as a result of uncertainties and variabilities in the model's input parameters. For the Monte Carlo simulation we pre-sampled 1,000 sets of random values for these parameters from their underlying distributions, and recalculated PECs and RQs for each set of values throughout the period 2031-2130. This produced a probability distribution for each PEC and RQ in each year, from which summary statistics (geometric mean, 25th and 75th percentiles) were derived.

Finally, we conducted a global sensitivity analysis using the moment-independent sensitivity importance measure proposed by Borgonovo[58,59] to rank all uncertain parameters in terms of their contribution to uncertainty in the resulting RQs in freshwater and natural soil compartments for all scales. We calculated these sensitivity measures using the *sensiFdiv* function in the *sensitivity* package for R developed by Iooss et al.[60]

5.3.Results and discussion

5.3.1.III-V/Si panel stock flows

The calculated stocks of III-V/Si panels installed and reaching their end-of-life in each year of the modelling period are shown in Figure 5-2. In Europe, carrying capacity is reached after the year 2110, while for Amsterdam it is reached at around the year 2080.

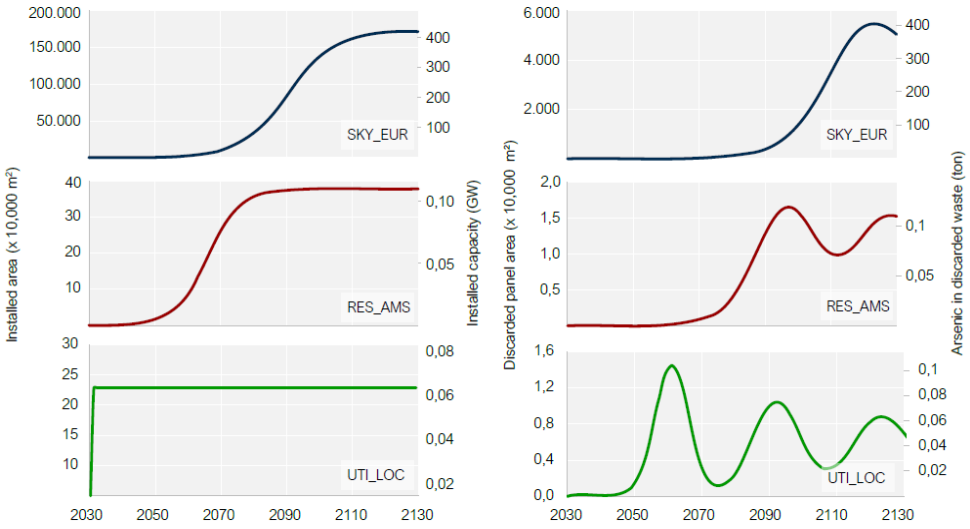

Figure 5-2 Projected III-V/Si PV demand (left) and discarded materials (right) for the three scales.

The steep ramp-up followed by stabilization in the demand growth curves (left) produces a ripple in the amount of PV materials that are available for recycling or final disposal at end-of-life (right). These oscillations are somewhat smoothened by uncertainty in the lifetime each cohort which varies around 30 years. As will be seen in sections 5.3.2 and 5.3.3, these oscillations in EOL stocks are then reflected in the emissions and PEC's.

5.3.2. III-V metals and metalloid emissions

The yearly emissions from the PV stocks during operation (USE) and disposal (EOL) in each scale are shown in Figure 5-3. These emissions were calculated for the single "base case" value for each parameter listed in Appendix Table A.4-1 (see Appendix Figure A.4-1 for the probabilistic results of the emissions model). Emissions from the use phase are several orders of magnitude lower than the emissions from the EOL phase, even when recycling is considered. At the largest scale (European continent, SKY_EUR), the quantity of arsenic emitted during the use phase starts stabilizing towards the end of the modelling period around 30 kg/year. In the regional (Amsterdam, RES_AMS) and local (UTI_LOC) scales, where they may be more concentrated, total emissions amount to grams which are then distributed over the respective areas of 220 km^2 and 16 km^2. This indicates that in all scenarios, the only relevant emissions are expected to occur at EOL.

In the end-of-life phase, total life-cycle emissions approach 1 ton/year in the SKY_EUR scenario at continental scale for the soil and air compartments. The quantities emitted to the air compartment are larger than quantities to soil at the beginning of the modelling period. This can be explained by the immediacy of the emissions during incineration: emissions which are not captured by the electrostatic precipitator during/after incineration, will be immediately released into the air compartment. On the other hand,

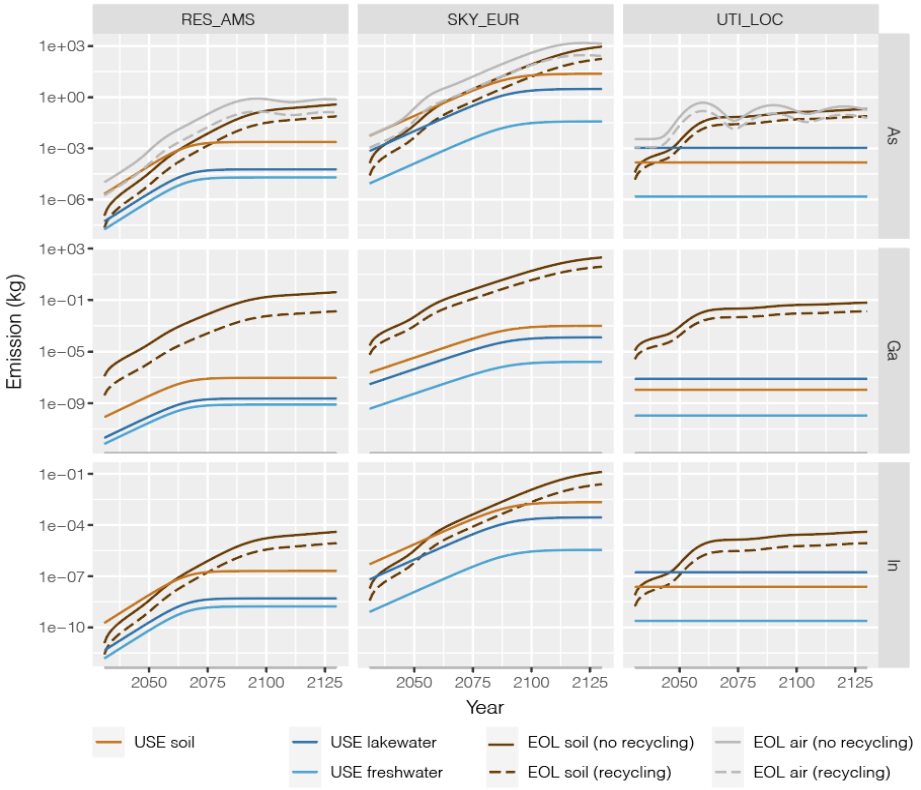

Figure 5-3 Life cycle emissions of III-V materials from III-V/Si PV installations in three different scenarios. EOL: End-of-Life phase; USE: Use phase.

emissions in a landfill are subject to a retardation factor represented by the large waste/leachate partitioning coefficients (K_w) of Equations 5-3 and 5-4. Towards the end of the modelling period, the emissions from landfill to the soil compartment are of similar magnitude than those to air in all scales. No air emissions are foreseen for gallium and indium due to their negligible volatilities.

5.3.3. Environmental fate of III-V metals and metalloids

The resulting PECs in soil and freshwater compartments are shown in Figure 5-4. At the end of the 100-year modelling period, the 75th percentile PEC of arsenic in freshwater in the local scale remains 1 to 2 orders of magnitude below the drinking water limits established by the World Health Organisation (without considering background levels or emissions). In the regional and continental scales, the PEC is 3-4 orders of magnitude lower. In soil, the 75th percentile PEC of arsenic is 5 orders of magnitude lower than the average concentration found in natural soils (1-40 mg/kg).[61] The geometric means are closer to the lower boundaries, suggesting skewed distributions with a long tail extending to the higher PEC values. The expected environmental concentrations of gallium and indium are in the nanogram range and lower, indicating negligible effects of this emissions from an ecological risk perspective.

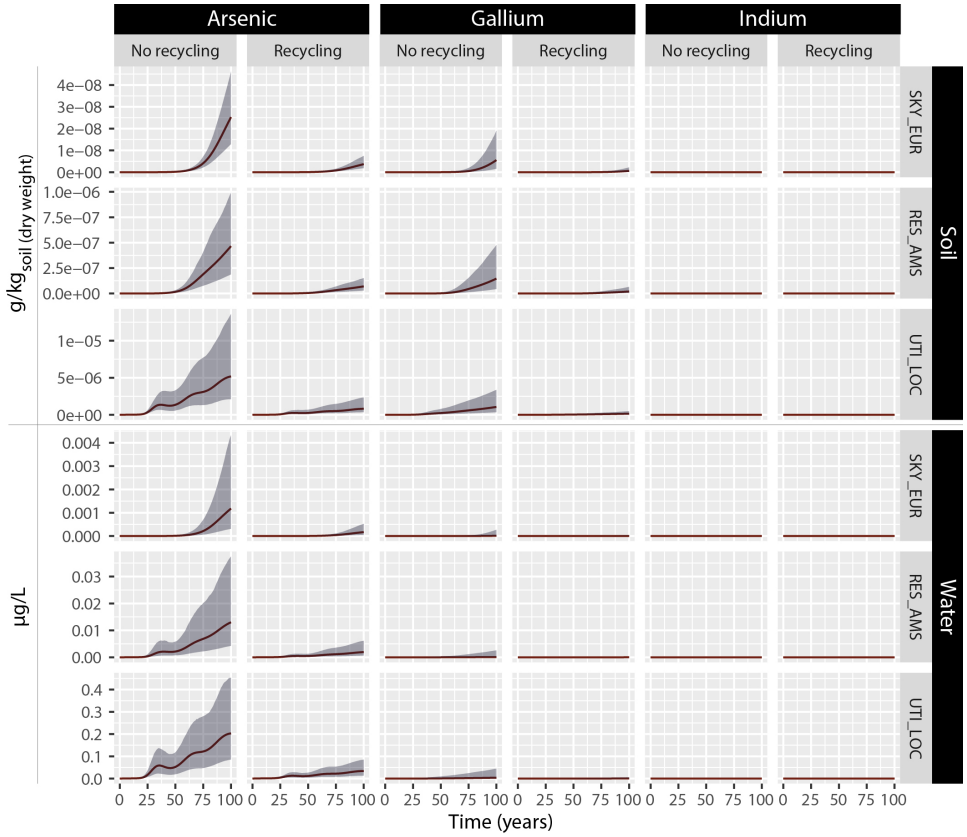

Figure 5-4 Predicted environmental concentrations of arsenic in soil and freshwater compartments in all scales, with and without recycling. The shaded area encloses the 25th and 75th percentiles and the solid line shows the geometric mean.

5.3.4. Ecological risks to freshwater and soil organisms

Figure 5-5 summarizes the RQs in the 100th year of simulation. As the scale volumes reduce in size (from continental to regional to local), the PECs and RQs increase. The local freshwater compartment presents the highest RQ for arsenic at ca. 0.1 for the upper range.

This could become a potential hotspot which may require consideration against background arsenic concentrations in the event a similar deployment is planned. The risk quotients for all other scales, compartments and metals are below 0.01. In all cases, recycling of the III-V content of the cells would reduce risks by one order of magnitude.

For the worst-case local scenario conditions for arsenic in which RQ approaches 0.1, some of the underlying assumptions merit further inspection with the aim of identifying potential risk attenuating mechanisms. A key starting assumption was that all emitted arsenic dissolves to its most toxic ion, arsenite (As(III)), which is assumed to persist as such.

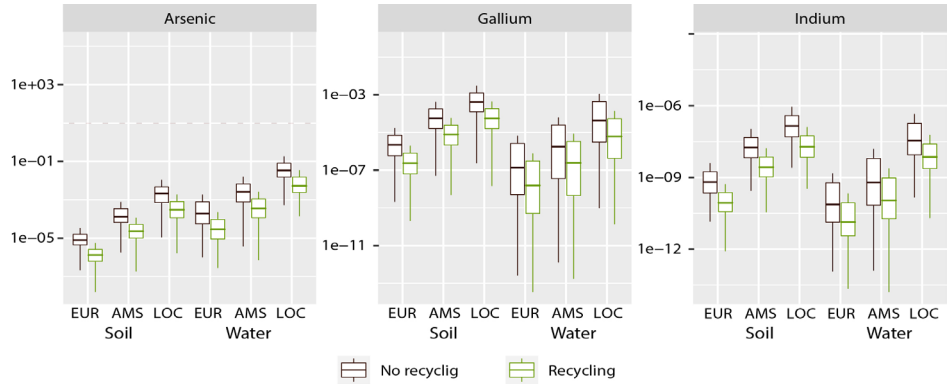

Figure 5-5 Risk Quotients for arsenic, gallium and indium in soil and freshwater compartments in all scales, with and without recycling.

However, arsenic undergoes several transformation processes which result in arsenate ions (As(V)) or even less toxic methylated organic forms.[62,63] The PNEC for As(III) is approximately 5 times lower than for As(V) in plant species.[61] A study of landfill leachate in Nordic countries found that arsenic in leachate is typically 80% arsenate, 10% arsenite and the rest is methylated.[64] Even lower percentages of As(III) (<5%) and higher amounts of methylated forms were reported by Pinel-Raffaitin and colleagues in landfill leachates sampled in France.[63]

In situ mechanisms to address As(III) mobilization in leakage from cracked panels during operation may be implemented as an additional precaution, especially in floating PV plants. Shumlas et al.[65], for example, reported accelerated oxidation of As(III) to As(V) when exposed to sunlight on layered manganese oxide. While such applications were developed for wastewater treatment in the case of arsenic, *in situ* mitigation concepts have already been proposed for perovskite PV cells where accidental lead leakage is immediately sequestered by lead-absorbing coatings.[66]

5.3.5. Sensitivity ranking of variable and uncertain parameters

The sensitivity rankings for all uncertain and variable model inputs in the integrated model and for all scales and compartments are shown in Figure 5-6. The most sensitive parameters are the waste/leachate partitioning coefficient in the landfill, the landfill cell depth, the fraction of vapourised arsenic captured in the incinerator's ESP, and the fraction of PV collected for recycling. For the landfill partitioning coefficient, the range of possible values spans several orders of magnitude.[67] It is likely that a large part of this dispersion is irreducible due to widely different landfill chemistries and environmental conditions that can be encountered. Further studying of the specific behaviour of arsenic in waste when exposed to leachate can however reduce the uncertainty. This has already been strongly advocated by Söderberg et al.[68] who reviewed 245 articles on soil/solution partitioning of metals in different media and found that none posterior to the EPA report[67] of 2005 investigated this parameter in waste disposal systems.

Figure 5-6 Sensitivity ranking of model parameters. L: local scale, R: regional scale, C: continental scale.

It is also noteworthy that despite the complexity and spatial dependency of the fate model, most of the parameters in this model component ranked low in terms of their contribution to uncertainty in the risk quotient. The sensitivity hotspots are clearly found in the EOL phase emissions model.

5.3.6. Recommendations for safe and sustainable III-V/Si PV installations

The most influential parameters identified in the global sensitivity analysis can offer opportunities to improve the design, not only of the photovoltaic cell, but of the configuration of large-scale deployments and the ancillary/complementary technological systems.

Waste/leachate partitioning coefficient. Despite its large variability, this highly influential factor can be addressed to some extent by controlling landfill chemistry, especially the pH of the leachate. It is likely that a construction and demolition (CDW) waste landfill with low organic waste content will produce leachate in higher pH ranges than a municipal solid waste (MSW) landfill where organic matter is being degraded and more acidic conditions emerge. Reaction of the ethyl vinyl acetate (EVA) encapsulation in PV panels with infiltrated water in the landfill may also produce acidic conditions, even in CDW landfills, by formation of acetic acid on the surface of discarded PV waste. Thus, delamination prior to disposal and/or replacement of the EVA encapsulation for alternative materials[69] in the panel's design may further reduce risks. This measure could also reduce leakage during operation of cracked panels, however the contribution of this release mechanism to the overall risk is already negligible.

Landfill depth. Stacking discarded PV waste in landfills more vertically rather than horizontally can have a significant retardation factor. Figure 5-7 shows the shift in the distribution curve of arsenic emissions to soil after the landfill depth is fixed at its higher range (10 m). The distribution is shifted significantly to the left and its tail size reduced.

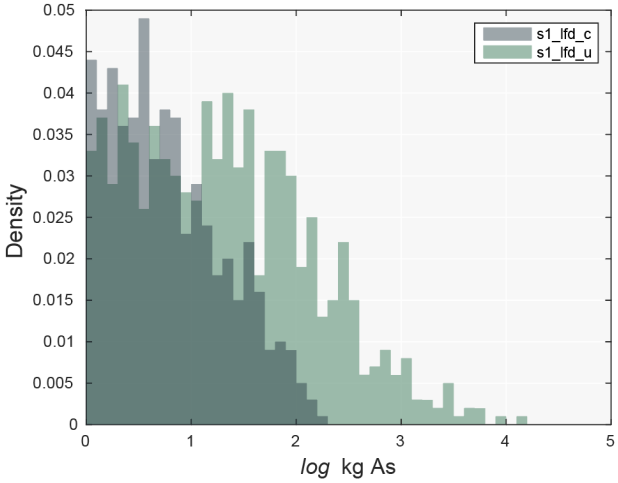

Figure 5-7 Change in distribution of arsenic emissions to soil (s1_lfd_u) as a result of fixing parameter landfill depth at lf.d = 10 m (s1_lfd_c).

Incinerator abatement efficiency (electrostatic precipitator). The fraction of vapourised arsenic that gets captured in the incinerator's electrostatic precipitator (thus prevented from direct release to the air compartment), also has an important influence. Even though the abatement efficiency range (98-99.9%) left small room for improvement, the results suggest that efforts to implement best available practice and marginal further improvements in abatement efficiency can result in noticeable risk reductions.

PV collection for recycling rate. By reintroducing III-V materials in PV waste into new economic products, they are effectively prevented from being released into the environment. The analysis not only showed an order of magnitude difference between the recycling and no-recycling scenario, but within the recycling scenario any efforts to increase collection above 85% will also result in important risk reductions.

The global sensitivity analysis also reveals where mitigation mechanisms may not be as effective in relation to the effort/cost required to implement them. For example, reducing arsenic content of the cells in the design and manufacturing within what is feasible will not have a noticeable effect on the risk profile of the III-V/Si technology. The same applies to measures to further reduce the cracking of panels – the use phase emissions are already too low to offer significant risk reduction.

5.3.7. Critical reflection on limitations and directions for future research

The integrated model we developed is complex in that it incorporates numerous interconnected cause-effect mechanisms to ensure all relevant factors are given consideration. Producing the data for such a model can be very time consuming, if the data is available at all. Therefore, some important assumptions and rough estimates were necessarily made. First, while the underlying landfill model is a good approximation for a monofill, the waste/leachate partitioning values (K_w) from EPA we used were taken from municipal solid waste (MSW) landfills, which will have phases where leachate has lower pH. This may significantly accelerate the release of arsenic from PV waste to the leachate. Second, we opted not to include a detailed speciation model for the dissolution of III-V species during use phase when exposed to acid rain or acetic acid attack. These models can increase the complexity of the assessment significantly, and they depend on a very large variability of water and waste chemistries which are difficult to determine at this stage. Given that the use phase emissions were considerably lower than the EOL emissions we decided to make conservative assumptions in this respect, although this may be an important aspect to incorporate if more detailed risk assessments are needed. Third, the dynamic emissions we calculated are largely dependent on the demand scenarios, more specifically the growth rates assumed for PV deployment (and the assumption of logistic growth curves). The market dynamics for PV are difficult to predict, with many forecasts having proved overly pessimistic in recent years.[70] Further coupling and updating of expected PV growth rates (specifically for III-V/Si markets) may shift the time-dependent results in a way that has important implications.

5.4. Conclusions

Our assessment indicates that the ecological risks from III-V materials emissions throughout the lifetime of III-V/Si PV panels do not pose a cause for concern, even under the worst-case situation modelled in the local scale. The main source of potentially toxic releases would be the above-ground disposal of III-V/Si cells in landfills. We find that the relevant increases in concentrations occur mostly in soil, while the contribution to the freshwater compartment was negligible across all scales. In soil, the mobility of III-V materials is very low, and releases will be diluted on the order of hundreds or thousands of years. Tighter regulations for landfill containment and monitoring systems will dilute these processes further. In the case of gallium and indium, these elements have much lower reactivity, so the emissions that do occur will have negligible effects. Nevertheless, at smaller scales with the co-occurrence of intense PV utilization and disposal, the risks may increase so that careful monitoring of the efficacy of control measures is required, particularly around landfill and incineration abatement, collection of used PV panels and increased recycling of arsenic. These factors will become increasingly important considering potential future expansion of markets for other arsenic containing electronic waste, such as that from discarded integrated circuits and LED diodes.

It is important to also consider that current social and regulatory trends in the European context have a clear direction towards reducing waste and increasing circularity of the economy. As an example, Germany sends less than 1% of its construction and demolition waste to landfills as of 2021.[71] European regulations have set demanding thresholds for electronic waste recycling, and numerous patents have demonstrated technologies for recovering materials from LEDs, integrated circuits, and photovoltaic devices with III-V materials grown via MOVPE. These recycling techniques can only be expected to become more efficient and cost-effective in time. Furthermore, the growing concerns over resource availability and supply risks of III-V materials like indium and gallium will provide further incentives. Considering these factors, a low-emission and low-risk scenario for the life cycle of future III-V/Si is likely.

As a final note, we highlight the value of the integrated model developed in this work for the early-stage assessment of chemical risks from emerging technologies. The model can be readily extended to other technologies beyond PV. In the past, such complex integrated models have seldom been applied at early R&D stages because of the time consuming and significant effort to construct and set up the models and the numerous uncertainties faced. But the framework and calculation algorithms we have made available make the rapid screening of different scenarios possible, while preserving the complexity and wide variety of influential factors found in real life. Furthermore, it is an ideal tool to prioritize research and data collection on influential factors during subsequent R&D stages.

References

1. Lazard. *Lazard's Levelized Cost of Energy Analysis - Version 12.0*. https://www.lazard.com/media/450784/lazards-levelized-cost-of-energy-version-120-vfinal.pdf (2018).
2. Jager, W. Stimulating the diffusion of photovoltaic systems: A behavioural perspective. *Energy Policy* **34**, 1935–1943 (2006).
3. Leenheer, J., de Nooij, M. & Sheikh, O. Own power: Motives of having electricity without the energy company. *Energy Policy* **39**, 5621–5629 (2011).
4. European Chemicals Agency. Silicon - Registration Dossier. https://echa.europa.eu/registration-dossier/-/registered-dossier/16144/7/1 (2020).
5. Jain, N. & Hudait, M. K. III–V Multijunction Solar Cell Integration with Silicon: Present Status, Challenges and Future Outlook. *Energy Harvest. Syst.* **1**, 121–145 (2014).
6. Dimroth, F. III-V Solar Cells - Materials, Multi-Junction Cells - Cell Design and Performance. in *Photovoltaic Solar Energy* 371–382 (John Wiley & Sons, Ltd, 2017). doi:10.1002/9781118927496.ch34.
7. Cariou, R. *et al.* III-V-on-silicon solar cells reaching 33% photoconversion efficiency in two-terminal configuration. *Nat. Energy* **3**, 326–333 (2018).
8. Essig, S. *et al.* Raising the one-sun conversion efficiency of III-V/Si solar cells to 32.8% for two junctions and 35.9% for three junctions. *Nat. Energy* **2**, 17144 (2017).
9. Lee, K. H. *et al.* Assessing material qualities and efficiency limits of III–V on silicon solar cells using external radiative efficiency. *Prog. Photovoltaics Res. Appl.* **24**, 1310–1318 (2016).
10. Arvidsson, R. *et al.* Environmental Assessment of Emerging Technologies: Recommendations for Prospective LCA. *J. Ind. Ecol.* **22**, 1286–1294 (2018).
11. Hetherington, A. C., Borrion, A. L., Griffiths, O. G. & McManus, M. C. Use of LCA as a development tool within early research: Challenges and issues across different sectors. *Int. J. Life Cycle Assess.* **19**, 130–143 (2014).
12. van der Giesen, C., Cucurachi, S., Guinée, J., Kramer, G. J. & Tukker, A. A critical view on the current application of LCA for new technologies and recommendations for improved practice. *J. Clean. Prod.* **259**, 120904 (2020).
13. Blanco, C. F., Cucurachi, S., Peijnenburg, W. J. G. M., Beames, A. & Vijver, M. G. Are Technological Developments Improving the Environmental Sustainability of Photovoltaic Electricity? *Energy Technol.* 1901064 (2020) doi:10.1002/ente.201901064.
14. Blanco, C. F. *et al.* Environmental impacts of III–V/silicon photovoltaics: life cycle assessment and guidance for sustainable manufacturing. *Energy Environ. Sci.* **13**, 4280–4290 (2020).

15. Sleeswijk, A. W., Heijungs, R. & Erler, S. T. Risk Assessment and Life-cycle Assessment: Fundamentally different yet reconcilable. *Greener Manag. Int.* (2003).

16. Guinée, J. B., Heijungs, R., Vijver, M. G. & Peijnenburg, W. J. G. M. Setting the stage for debating the roles of risk assessment and life-cycle assessment of engineered nanomaterials. *Nat. Nanotechnol.* **12**, 727–733 (2017).

17. Zimmermann, Y. S., Schäffer, A., Corvini, P. F. X. & Lenz, M. Thin-film photovoltaic cells: Long-term metal(loid) leaching at their end-of-life. *Environ. Sci. Technol.* **47**, 13151–13159 (2013).

18. Celik, I., Song, Z., Heben, M. J., Yan, Y. & Apul, D. S. Life cycle toxicity analysis of emerging PV cells. in *Conference Record of the IEEE Photovoltaic Specialists Conference* vols 2016-Novem 3598–3601 (IEEE, 2016).

19. Babayigit, A., Ethirajan, A., Muller, M. & Conings, B. Toxicity of organometal halide perovskite solar cells. *Nat. Mater.* **15**, 247 (2016).

20. Zeng, C. *et al.* Ecotoxicity assessment of ionic As(III), As(V), In(III) and Ga(III) species potentially released from novel III-V semiconductor materials. *Ecotoxicol. Environ. Saf.* **140**, 30–36 (2017).

21. Collingridge, D. *The social control of technology*. (Frances Pinter, 1980).

22. U.S. Environmental Protection Agency. *Risk Assessment Forum White Paper: Probabilistic Risk Assessment Methods and Case Studies*. http://epa.gov/raf/prawhitepaper/index.htm (2014).

23. Shell International B.V. Sky Scenario. *Shell Scenarios SKY Meeting the Goals of the Paris Agreement* https://www.shell.com/energy-and-innovation/the-energy-future/scenarios/shell-scenario-sky.html (2018).

24. IEA. *The Role of Critical Minerals in Clean Energy Transitions*. (2021).

25. City of Amsterdam. Policy: Renewable energy. *Policy: Sustainability and energy* https://www.amsterdam.nl/en/policy/sustainability/renewable-energy/.

26. Jaxa-Rozen, M. & Trutnevyte, E. Sources of uncertainty in long-term global scenarios of solar photovoltaic technology. *Nat. Clim. Chang.* **11**, 266–273 (2021).

27. Deetman, S., Pauliuk, S., van Vuuren, D. P., van der Voet, E. & Tukker, A. Scenarios for Demand Growth of Metals in Electricity Generation Technologies, Cars, and Electronic Appliances. *Environ. Sci. Technol.* **52**, 4950–4959 (2018).

28. Pauliuk, S. & Heeren, N. ODYM—An open software framework for studying dynamic material systems: Principles, implementation, and data structures. *J. Ind. Ecol.* **24**, 446–458 (2020).

29. van der Voet, E., Kleijn, R., Huele, R., Ishikawa, M. & Verkuijlen, E. Predicting future emissions based on characteristics of stocks. *Ecol. Econ.* **41**, 223–234 (2002).

30. Köntges, M. *et al. Review of Failures of Photovoltaic Modules*. https://iea-pvps.org/wp-content/uploads/2020/01/IEA-PVPS_T13-01_2014_Review_of_Failures_of_Photovoltaic_Modules_Final.pdf (2014).

31. Fraunhofer ISE. SiTaSol: Application relevant validation of c-Si based tandem solar cell processes. https://sitasol.com/.

32. Licht, C., Peiró, L. T. & Villalba, G. Global Substance Flow Analysis of Gallium, Germanium, and Indium: Quantification of Extraction, Uses, and Dissipative Losses within their Anthropogenic Cycles. *J. Ind. Ecol.* **19**, 890–903 (2015).

33. Celik, I., Song, Z., Phillips, A. B., Heben, M. J. & Apul, D. Life cycle analysis of metals in emerging photovoltaic (PV) technologies: A modeling approach to estimate use phase leaching. *J. Clean. Prod.* **186**, 632–639 (2018).

34. Noyes, A. A. & Whitney, W. R. The rate of solution of solid substances in their own solutions. *J. Am. Chem. Soc.* **19**, 930–934 (1897).

35. Mathai, A. M., Moschopoulos, P. & Pederzoli, G. Random points associated with rectangles. *Rend. del Circ. Mat. di Palermo* **48**, 163–190 (1999).

36. European Parliament; Council of the European Union. *Directive 2012/19/EU of the European Parliament and of the Council of 4 July 2012 on waste electrical and electronic equipment (WEEE)*. (2012). doi:10.3000/19770677.L_2012.197.eng.

37. Van Den Bossche, A., Vereycken, W., Vander Hoogerstraete, T., Dehaen, W. & Binnemans, K. Recovery of Gallium, Indium, and Arsenic from Semiconductors Using Tribromide Ionic Liquids. *ACS Sustain. Chem. Eng.* **7**, 14451–14459 (2019).

38. Maarefvand, M., Sheibani, S. & Rashchi, F. Recovery of gallium from waste LEDs by oxidation and subsequent leaching. *Hydrometallurgy* **191**, (2020).

39. Zhan, L., Xia, F., Xia, Y. & Xie, B. Recycle Gallium and Arsenic from GaAs-Based E-Wastes via Pyrolysis-Vacuum Metallurgy Separation: Theory and Feasibility. *ACS Sustain. Chem. Eng.* **6**, 1336–1342 (2018).

40. Jung, C. ., Matsuto, T., Tanaka, N. & Okada, T. Metal distribution in incineration residues of municipal solid waste (MSW) in Japan. *Waste Manag.* **24**, 381–391 (2004).

41. Hasselriis, F. & Licata, A. Analysis of heavy metal emission data from municipal waste combustion. *J. Hazard. Mater.* **47**, 77–102 (1996).

42. Blasenbauer, D. *et al.* Legal situation and current practice of waste incineration bottom ash utilisation in Europe. *Waste Manag.* **102**, 868–883 (2020).

43. U.S. Environmental Protection Agency Office of Solid Waste. *EPA's Composite Model for Leachate Migration with Transformation Products (EPACMTP) Technical Background Document*. (2003).

44. European Chemicals Agency. *Guidance on Information Requirements and Chemical Safety Assessment - ECHA*. https://echa.europa.eu/guidance-documents/guidance-on-information-requirements-and-chemical-safety-assessment (2011).

45. Jensen, H., Gaw, S., Lehto, N. J., Hassall, L. & Robinson, B. H. The mobility and plant uptake of gallium and indium, two emerging contaminants associated with electronic waste and other sources. *Chemosphere* **209**, 675–684 (2018).

46. Hollander, A., Schoorl, M. & van de Meent, D. SimpleBox 4.0: Improving the model while keeping it simple…. *Chemosphere* **148**, 99–107 (2016).

47. Vermeire, T. G. *et al.* European Union System for the Evaluation of Substances (EUSES). Principles and structure. *Chemosphere* **34**, 1823–1836 (1997).

48. City of Amsterdam. Maps Data. *2019* https://maps.amsterdam.nl/open_geodata/?LANG=en.

49. The Royal Netherlands Meteorological Institute (KNMI). Klimatologie - Metingen en waarnemingen. https://www.knmi.nl/nederland-nu/klimatologie-metingen-en-waarnemingen.

50. Schoorl, M., Hollander, A. & van de Meent, D. *SimpleBox 4.0 A multimedia mass balance model for evaluating the fate of chemical substances.* https://www.rivm.nl/bibliotheek/rapporten/2015-0161.pdf (2015).

51. van de Meent, D., Zwart, D. & Posthuma, L. Screening-Level Estimates of Environmental Release Rates, Predicted Exposures, and Toxic Pressures of Currently Used Chemicals. *Environ. Toxicol. Chem.* **39**, 1839–1851 (2020).

52. European Chemicals Agency. Gallium - Registration Dossier - ECHA. *Gallium* https://echa.europa.eu/registration-dossier/-/registered-dossier/23228/6/2/4.

53. European Chemicals Agency. Indium - Registration Dossier - ECHA. *Indium* https://echa.europa.eu/registration-dossier/-/registered-dossier/22264.

54. European Chemicals Agency. Arsenic - Registration Dossier - ECHA. *Arsenic* https://echa.europa.eu/registration-dossier/-/registered-dossier/22366.

55. ChemSafetyPro. How to Calculate Predicted No-Effect Concentration (PNEC).

56. Su, J. Y., Syu, C. H. & Lee, D. Y. Growth inhibition of rice (Oryza sativa L.) seedlings in Ga- and In-contaminated acidic soils is respectively caused by Al and Al + In toxicity. *J. Hazard. Mater.* **344**, 274–282 (2018).

57. Firestone, M. *et al. Guiding Principles for Monte Carlo Analysis - Technical Panel.* https://www.epa.gov/risk/guiding-principles-monte-carlo-analysis (1997).

58. Borgonovo, E. A new uncertainty importance measure. *Reliab. Eng. Syst. Saf.* **92**, 771–784 (2007).

59. Plischke, E. & Borgonovo, E. Fighting the Curse of Sparsity: Probabilistic Sensitivity Measures From Cumulative Distribution Functions. *Risk Anal.* risa.13571 (2020) doi:10.1111/risa.13571.

60. Iooss, B., Da Veiga, S., Janon, A. & Pujol, G. Global Sensitivity Analysis of Model Outputs. (2021).

61. World Health Organization. *Environmental Health Criteria 224 Arsenic and Arsenic Compounds Second Edition.* (2001).

62. Jain, C. K. & Ali, I. Arsenic: Occurrence, toxicity and speciation techniques. *Water Res.* **34**, 4304–4312 (2000).

63. Pinel-Raffaitin, P., Le Hecho, I., Amouroux, D. & Potin-Gautier, M. Distribution and Fate of Inorganic and Organic Arsenic Species in Landfill Leachates and Biogases. *Environ. Sci. Technol.* **41**, 4536–4541 (2007).

64. Harstad, K. *Handling and assessment of leachates from municipal solid waste landfills in the Nordic countries*. (2007). doi:https://doi.org/https://doi.org/10.6027/TN2006-594.

65. Shumlas, S. L. *et al.* Oxidation of arsenite to arsenate on birnessite in the presence of light. *Geochem. Trans.* **17**, 5 (2016).

66. Li, X. *et al.* On-device lead sequestration for perovskite solar cells. *Nature* **578**, 555–558 (2020).

67. Allison, J. D. & Allison, T. L. *Partitioning Coefficients for Metals in Surface Water, Soil and Waste*. https://cfpub.epa.gov/si/si_public_record_report.cfm?Lab=NERL&dirEntryId=135783 (2005).

68. Uddh Söderberg, T. *et al.* Metal solubility and transport at a contaminated landfill site – From the source zone into the groundwater. *Sci. Total Environ.* **668**, 1064–1076 (2019).

69. Adothu, B. *et al.* Newly developed thermoplastic polyolefin encapsulant–A potential candidate for crystalline silicon photovoltaic modules encapsulation. *Sol. Energy* **194**, 581–588 (2019).

70. Creutzig, F. *et al.* The underestimated potential of solar energy to mitigate climate change. *Nat. Energy* **2**, 17140 (2017).

71. Ferdous, W. *et al.* Recycling of landfill wastes (tyres, plastics and glass) in construction – A review on global waste generation, performance, application and future opportunities. *Resour. Conserv. Recycl.* **173**, 105745 (2021).